Atmósfera (1995), **8**, *pp. 99-114*

Prevailing anomaly patterns of the Global Sea Surface temperatures and tropospheric responses

ERNEST C. KUNG and JONQ-GONG CHERN

University of Missouri-Columbia Columbia, Missouri 65211, USA

(Manuscript received Nov. 29, 1994; accepted Feb. 7, 1995)

RESUMEN

Se presenta una clasificación sinóptica de los campos de anomalías observadas de las temperaturas superficiales del mar (SST) globales a nivel mensual para el periodo 1955-1993. Los campos de anomalías mensuales se agrupan en siete tipos característicos. Las respuestas troposféricas en el Hemisferio Norte a aquellos tipos de SST se describen en función de los campos a 700, 500 y 300 Hpa del geopotencial de altitud (Z), así como los campos de espesores de 700-500 Hpa y 500-300 Hpa.

Cada tipo de anomalías de temperaturas superficiales del mar está asociado con un campo de anomalía diferente del geopotencial (Z) cuyos patrones característicos son congruentes desde la baja hasta la alta troposfera.

Las fluctuaciones climáticas durante las cuatro últimas décadas son dibujadas por los patrones predominantes del SST mensuales.

El predominio de los campos de anomalías tipo El Niño-Oscilación Suriana (ENSO) durante los años recientes, caracteriza el modo reinante en la actualidad. Se presentan las componentes principales de los campos de SST anómalos, para el periodo julio de 1991 a diciembre de 1993, para describir los patrones de SST tipo ENSO, recientes.

Se examina el posible enfoque del Indice del Niño (ENI) aquí definido en la proyección a largo plazo de la circulación atmosférica, con correlación cruzada entre los ENIs y la circulación troposférica subsiguiente.

La utilidad del ENIs como predictor está indicada a nivel estacional.

ABSTRACT

A synoptic classification of observed anomaly fields of the monthly global sea surface temperatures (SSTs) is presented for the period of 1955-1993. The monthly anomaly fields are grouped into characteristic seven types. The Northern Hemisphere tropospheric responses to these SST types are described in terms of the geopotential height (Z) fields at 700, 500, and 300 mb and thickness fields for 700-500 mb and 500-300 mb. Each type of SST anomalies is associated with a distinct anomaly field of Z, whose characteristic patterns are consistent from the lower to upper troposphere.

The climatic variations during the past four decades are depicted by the prevailing monthly SST patterns. The dominance of the El Niño - Southern Oscillation (ENSO) type anomaly fields during the recent years characterizes the climatic mode prevalent at present. Principal components of the SST anomaly fields during the period of July 1991 to December 1993 are presented for the description of the recent ENSO type SST patterns. A possible utilization of defined El Niño Index (ENI) in the long-range projection of the atmospheric circulation is examined with cross-correlation between the preceding ENIs and following tropospheric circulation. The usefulness of ENIs as a predictor is indicated at the seasonal range.

I. Introduction

In the preceding paper (Kung *et al.*, 1994) we presented a principal component analysis on the large-scale modes of variations in the global sea surface temperatures (SSTs) and Northern Hemisphere tropospheric circulation for the 38-year period from 1955-1992. The cross-correlations of SST components with the tropospheric circulation so presented in the paper suggest a useful predictability of the tropospheric circulation in reference to SST anomalies.

As the major principal components of SSTs are shown in Kung *et al.* (1994) to have controlling effects on the concurrent and following Northern Hemispheric circulation with a lead time of one to three seasons, it will be interesting to establish synoptic categories of SST anomaly patterns for readily recognizing the prevailing SST patterns without invoking principal component analysis. In this study the observed monthly anomaly fields of the global SSTs during the 39-year period of 1955-1993 are classified into seven characteristic types. The climate variations as shown in the classification of monthly SSTs are examined. The Northern Hemisphere circulations associated with these SST types are studied in terms of geopotential height fields (Z) at 700, 500, and 300 mb, and 700-500 mb and 500-300 mb thickness fields. Further, the dominance of the El Niño-Southern Oscillation (ENSO) since the later 1970s to present is examined with the principal components of SSTs during the most recent thirty months from July 1991 to December 1993, when the most recent major ENSO episode overwhelmed the Northern Hemisphere circulation. An El Niño Index (ENI) is defined in this study as the weighted mean of the coefficients of the 1st and 2nd components of SSTs by the respective variances, and its utilities in the long-range prediction of the atmospheric circulation is examined.

The SST and upper-air data and method of principal component analysis are as described in Kung *et al.* (1994) and will not be repeated here. However, it should be noted that new data of 1993 have been added to the original database of 1955-1992. The monthly SST anomaly fields as used for their synoptic classification are in reference to the 39-year means of monthly SSTs during 1955-1993. The results of principal component analysis reported in Kung *et al.* (1994) are used to compute ENIs weighted by variances of the 1st and 2nd components.

2. Synoptic classification of SST anomaly patterns

Through the objective application of the clustering method (e.g., Fukunaga 1972) and the manual inspection of monthly SST anomaly patterns during the entire period of 1955-92, seven types of anomaly distribution are recognized, namely Type A, B, C, D, E, F and G. These types are illustrated in Figure 1 in terms of average monthly anomaly patterns of individual types during the entire period. In classifying the SST anomaly pattern, special care is taken so that each monthly pattern belongs to a distinct group, and the frequency distribution is comparable among these groups. The identification of anomaly types involves a degree of subjectivity. However, the types as illustrated in Figure 1 are distinctive, and we also have not experienced difficulty in classifying individual monthly SST patterns into one of these seven categories.

Unlike the principal components which are expected to represent fundamental modes of variation, the synoptic classification as shown in Figure 1 may show interactive, intermediate and transitional modes as well as the fundamental modes. The F type, which is observed during ENSO episodes, reflects 1st and 2nd principal components of SSTs (Kung *et al.*, 1994) as we may appropriately define ENI by their coefficients. The C type is also observed during the ENSO episodes, but reflects the 2nd principal component only. The G type is essentially a reversed phase of F type with a greater intensity in the temperature gradient. The A type is characterized by the generally positive anomalies in the Northern Hemisphere and generally negative anomalies

in the Southern Hemisphere. The B type is characterized by the negative anomalies from the subtropics of the Southern Hemisphere to cover the entire Northern Hemisphere. The D and E types may be considered as intermediate or transitional types. The D type may be observed in the period with ENSO episodes. However, it is not as stable as F type, and the associated

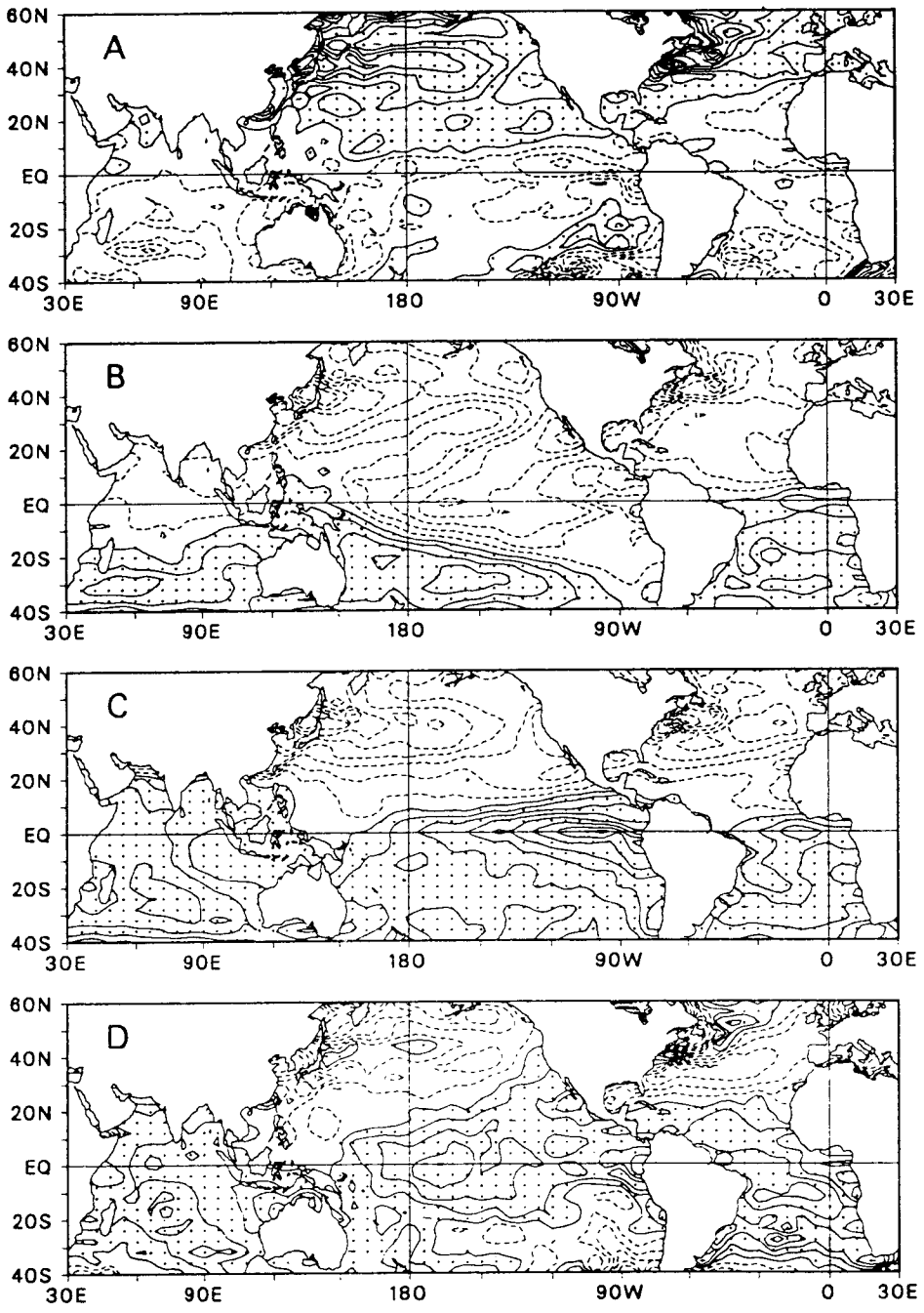

Figure 1

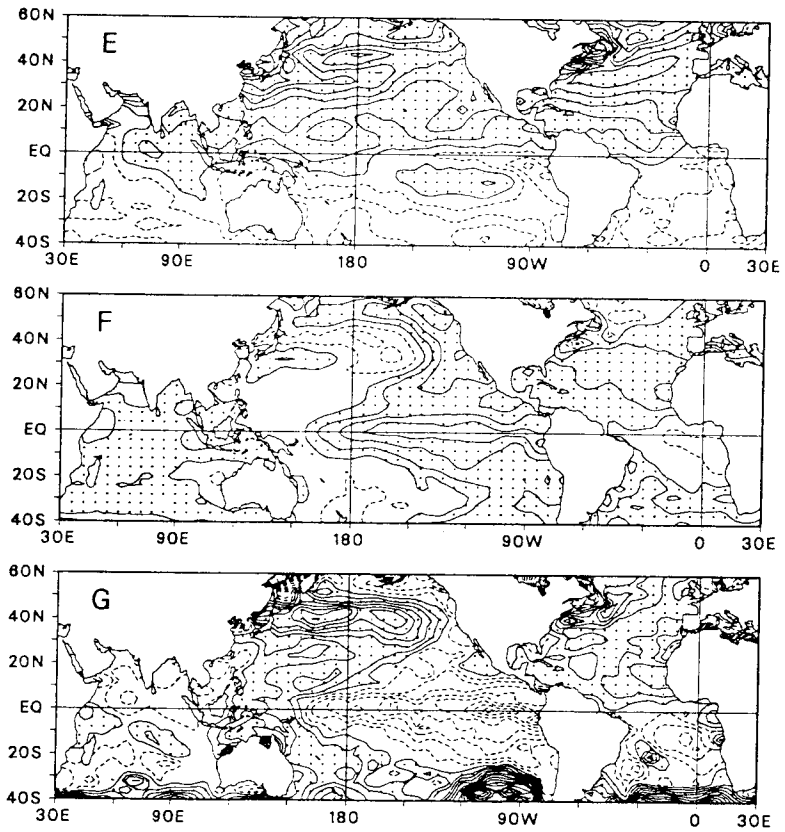

Fig. 1. Seven identified types of SST anomaly distribution for the period of 1955-93. Solid lines are for zero and positive, and dashed lines for negative. The contour interval is 0.2°C.

ENSO may be rather short lived. The type E is generally observed during the same general period when F type dominates (Tables 1 and 2), but is more transient in holding the pattern than the F type.

Table 1 lists the SST anomaly types of all months during the period of 1955-93. Table 2 further lists the annual frequency distribution of various types for the period. The period of 1955-93 is further divided into five sub-periods, as shown at the bottom of Table 2 according to the dominance of certain types of SST anomalies. In Tables 1 and 2 the shift of prevailing climatic patterns is clearly indicated in the transition of prevailing SST anomaly patterns. In the early part of the period in the 1950s and 1960s, we see frequent occurrences of types A, D and G, the North Pacific and Atlantic showing generally positive SST anomalies, although types D and G show areas of opposite signs. During the 1970s, we see frequent occurrences of types B and C which indicate a cooler North Pacific. From the late 1970s to the present we see a drastic increase of E and F types, along with the increase in reported ENSO episodes. Dominance of the ENSO mode since the late 1970s essentially characterizes the current prevailing climate pattern.

The decade-scale time variations of SSTs are recognized in various sources of observational records (Halpert *et al.*, 1994; World Meteorological Organization, 1991). However, at the present time the cause and mechanism of the SST variations are not well known in definitive terms (Houghton *et al.*, 1990, 1992). Whatever the physical explanations of SST variations are, it is important to recognize the long time scale and persistency of SST anomaly fields in refer-

ence to the much shorter characteristic time of the atmospheric general circulation. The long characteristic time of SSTs make them a viable predictor for the long-range forecasting of the atmospheric conditions.

Table 1. Types of monthly SST anomaly patterns during the period of 1955-93.

Year	JAN	FEB	MAR	APR	MAY	JUN	JUL	AUG	SEP	OCT	NOV	DEC
1955	A	A	A	A	A	A	A	A	A	G	G	G
1956	A	A	A	A	A	A	A	A	A	G	G	G
1957	G	A	A	A	A	F	F	F	F	F	F	D
1958	D	D	D	D	D	D	F	F	F	D	D	D
1959	D	D	D	D	D	D	A	A	A	A	A	A
1960	A	A	A	A	A	A	D	A	A	A	G	A
1961	A	A	A	A	A	A	A	A	A	A	G	G
1962	G	G	G	G	G	G	G	D	G	G	G	G
1963	A	A	D	D	D	D	D	D	D	D	D	D
1964	D	D	A	D	A	A	A	G	G	G	A	A
1965	A	A	A	A	A	A	A	F	F	F	F	F
1966	D	D	D	D	D	A	A	A	A	D	D	D
1967	A	A	A	A	A	A	A	A	A	A	A	A
1968	A	A	A	A	A	A	A	F	F	F	D	D
1969	D	D	D	D	D	F	D	E	E	E	D	D
1970	C	C	C	C	C	C	C	B	B	B	B	B
1971	B	B	B	C	B	B	B	B	B	B	B	B
1972	B	B	B	C	C	C	C	F	C	C	C	C
1973	C	C	C	B	B	B	B	B	B	B	B	B
1974	B	B	B	B	B	B	B	B	B	B	B	B
1975	B	B	B	B	B	B	B	B	B	B	B	B
1976	B	B	B	B	B	B	B	C	C	C	F	F
1977	C	C	C	B	B	E	E	E	E	E	C	F
1978	F	F	F	E	E	B	C	E	E	C	F	F
1979	C	C	C	C	C	C	F	F	F	F	F	F
1980	F	F	F	F	F	E	E	E	E	E	E	E
1981	F	F	F	C	C	E	E	E	E	E	E	E
1982	E	E	E	E	C	F	F	C	C	C	C	F
1983	C	F	F	F	F	F	F	E	E	C	E	E
1984	E	E	F	B	E	B	E	E	E	E	B	B
1985	B	B	B	B	B	E	E	E	E	E	E	E
1986	E	E	F	E	E	F	F	F	F	F	F	F
1987	F	F	E	E	F	C	F	E	F	E	F	F
1988	E	E	E	E	E	E	E	E	E	A	A	G
1989	G	G	G	G	F	F	E	E	E	E	F	F
1990	A	E	E	F	F	F	F	F	D	D	D	D
1991	D	F	F	C	C	E	E	E	E	F	F	F
1992	F	F	F	F	F	F	F	F	F	F	F	F
1993	F	F	F	F	F	F	F	F	D	F	F	F

Table 2. Annual frequency distribution of monthly SST anomaly types during the period of 1955-93.

YEAR/ PERIOD	A	B	C	D	E	F	G
1955	9						3
1956	9						3
1957	4			1		6	1
1958				9		3	
1959	6			6			
1960	10			1			1
1961	10						2
1962				1			11
1963	2			10			
1964	6			3			3
1965	7					5	
1966	4			8			
1967	12						
1968	7			2		3	
1969				8	3	1	
1970		5	7				
1971		11	1				
1972		3	8			1	
1973		9	3				
1974		12					
1975		12					
1976		7	3			2	
1977		2	4		5	1	
1978		1	2		4	5	
1979			6			6	
1980					7	5	
1981			2		7	3	
1982			5		4	3	
1983			2		4	6	
1984		4			7	1	
1985		5			7		
1986					4	8	
1987			1		4	7	
1988	2				9		1
1989					4	4	4
1990	1			4	2	5	
1991			2	1	4	5	
1992						12	
1993				1		11	
1955-62	48			18		9	21
1963-69	38			31	3	9	3
1970-75		52	19			1	
1976-83		10	24		31	31	
1984-93	3	9	3	6	41	53	5

3. Tropospheric circulation in response to SST anomaly fields

The anomaly fields of the tropospheric circulation associated with various anomaly types of SSTs are presented in Figures 2-4 in terms of anomaly fields of January Z at 700, 500 and 300 mb. Comparing Figures 2, 3 and 4, it is clear that each type of SST anomalies is associated with a distinct anomaly field of Z, and the anomaly fields of Z show the characteristic patterns through the troposphere from 700 mb to 300 mb.

With the A and E types of SSTs (Fig. 1) that show generally warm Northern Hemisphere oceans, particularly in the Pacific, the Northern Hemisphere circulation indicates enhancement and weakening at three locations: the Eurasian continent, North Pacific Ocean, and the eastern half of the North American continent and North Atlantic. This pattern is most clearly illus-

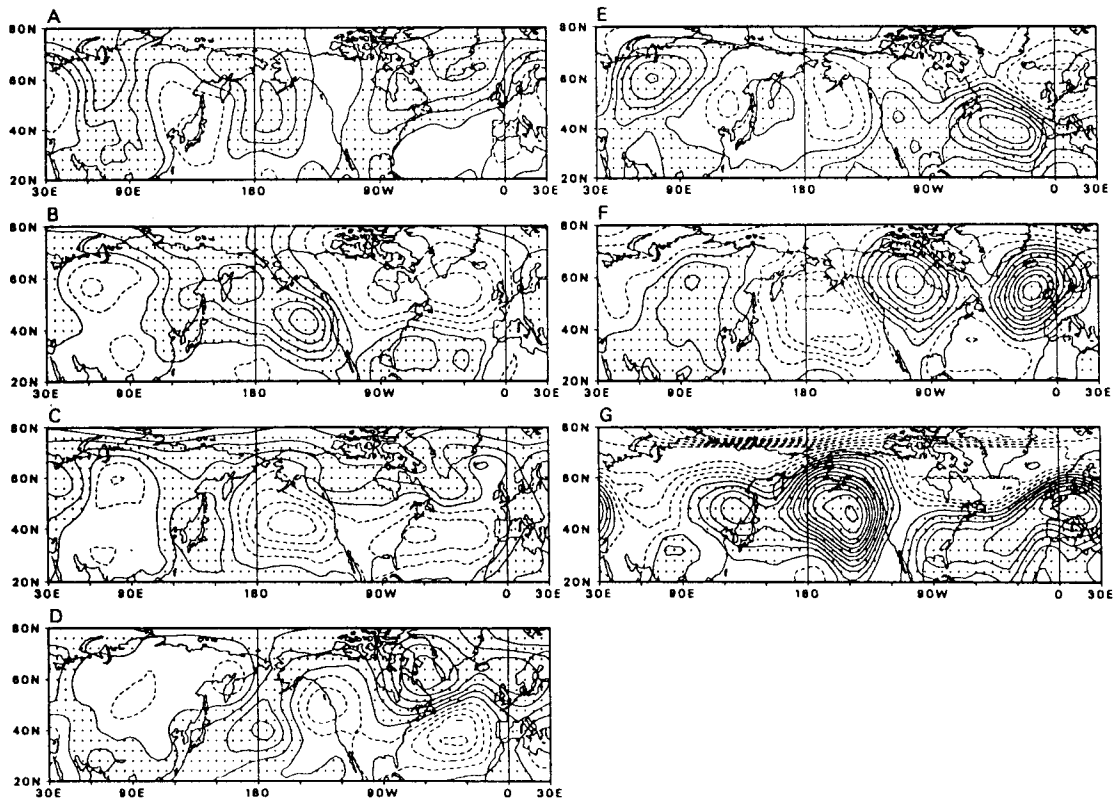

Fig. 2. Anomaly fields of January 700 mb Z associated with different types of SST anomalies during the period of 1955-93. Solid lines are for zero and positive, and dashed lines for negative. The contour interval is 10 m.

trated for A type, and is somewhat compromised for E type with weakening in the Pacific. As indicated in Figures 5-6, thermal fields as represented by anomaly fields of the January 500-700 mb thickness and 300-500 mb thickness reflect the anomalous heating under A and E types that in turn form the characteristic anomaly fields of Z in Figures 2-4. It is pointed out in Kung *et al.* (1993) that the *in site* warming over the Pacific and Atlantic may form the Pacific and Atlantic blockings. This argument is consistent with the anomalous high pressure component shown in the A and E types.

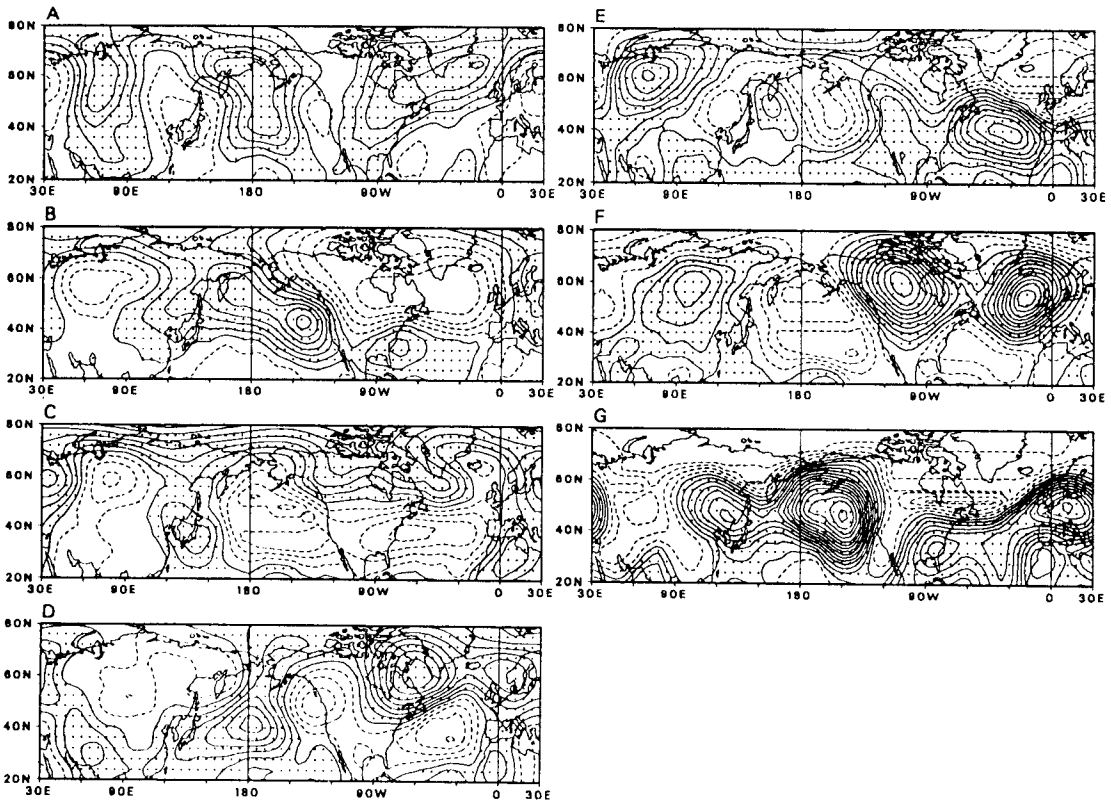

Fig. 3. As in Figure 2, but for 500 mb.

It is pertinent to note here that the baroclinic process by *in site* heating of the lower atmosphere is not the only cause of high pressure or ridge formation. As reported by Hartman and Ghan (1980), Kung and Baker (1986) and DaCamara *et al.* (1992), a large cold patch in the North Pacific or North Atlantic favors the development of high pressure blocking through the nonlinear wave-wave transformation of kinetic energy of baroclinic origin into the barotropic kinetic energy of planetary-scale waves. The B type is clearly a case. The general cooling in the Pacific results in the high pressure ridge over the Pacific north of 20°N. The source of the energy for nonlinear wave- wave interaction in the North Pacific is found in the sharp meridional gradient

of temperature in the lower latitudes of the Southern Hemisphere (Fig. 2). The type C shows general negative SST anomalies in both the North Pacific and Atlantic Oceans north of the tropical region, and we see high pressure in two areas: the Northwestern Pacific Ocean and eastern Asian continent, and the Northwestern Atlantic Ocean and Canada. The anomaly field of Z associated with type F is characterized by a positive area in the Asian continent and a negative area over the Pacific, and strong positive areas over the North American continent and North Atlantic. As the SST anomalies of type F are those of strong ENSO periods, the resulting anomaly field of Z is responsible to the anomalous storm tracks and Northern Hemispheric circulation which are observed during major ENSO episodes. The type D SSTs, also observed during ENSO, show a similar Z field to that of type F. However, the patterns are generally shifted to the east, reflecting a general cooling in both the North Pacific and Atlantic.

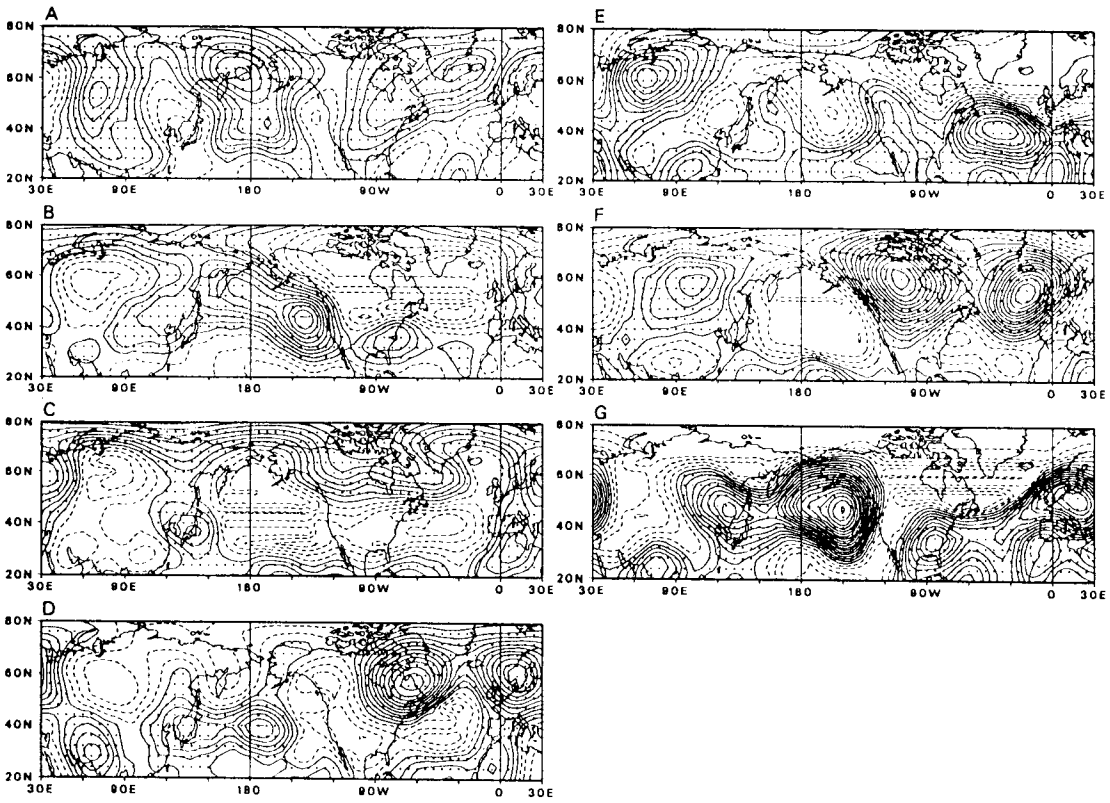

Fig. 4. As in Figure 3, but for 300 mb.

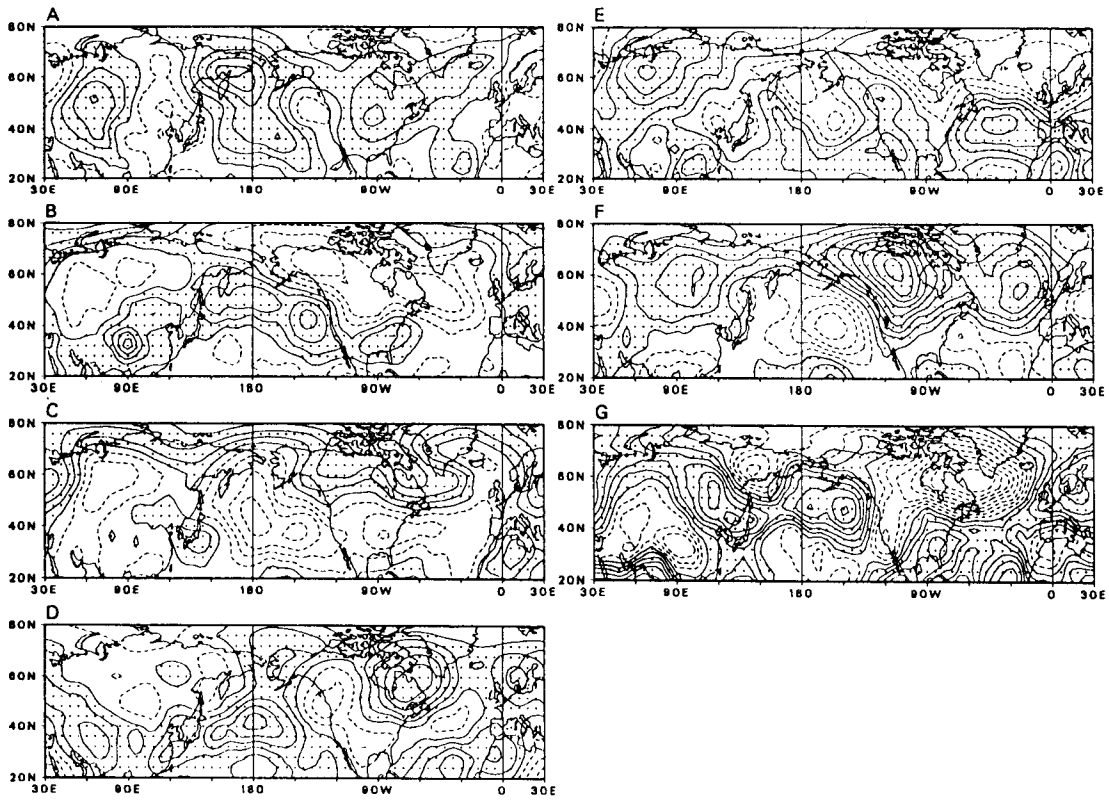

Fig. 5. Anomaly fields of January 500-700 mb thickness associated with different types of SST anomalies during the period of 1955-93. Solid lines are for zero and positive, and dashed lines for negative. The contour interval is 5 m.

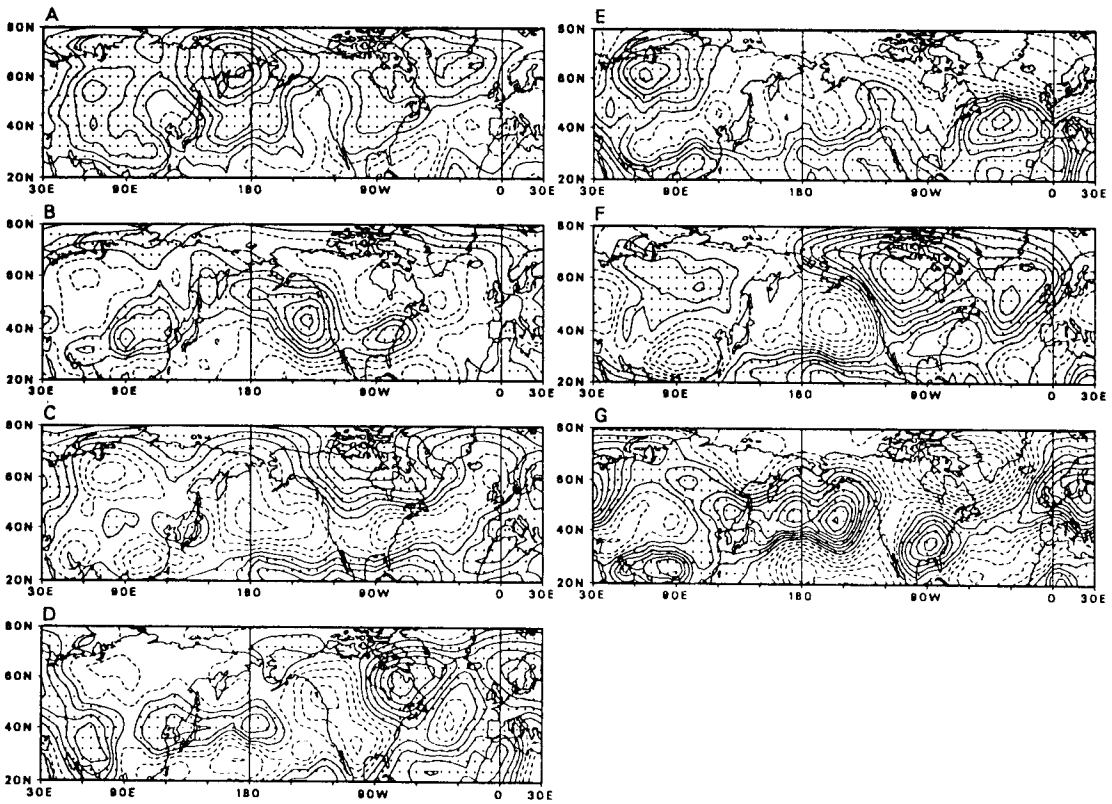

Fig. 6. As in Figure 5, but for January 300-500 mb thickness.

The type G with strong negative SST anomalies in the tropical eastern Pacific and tropical Atlantic shows very intense patterns of Z anomalies with double core positive areas in both the eastern and western halves of the Northern Hemisphere. The SST anomaly patterns (Fig. 1) indicate a strong meridional gradient of SSTs with an ample baroclinic source of energy in the Pacific. Apparently both the *in site* warming and nonlinear wave-wave energy transformation are working to form such intense anomalies of Z field.

The response of the tropospheric circulation to the lower boundary forcing of SSTs is expected to be different in the summer from the winter circulation. In the summer the circulation is weak and the patterns are more fragmental (Kung *et al.*, 1994) because the meridional temperature gradient is less and the source of the baroclinic energy is limited. The response of the summer circulation to various SST types is illustrated in Figures 7 and 8 in terms of July 300-700 mb thickness anomalies and resulting 300 mb anomaly fields of Z. Despite the more fragmental patterns and shift of phases, some winter characteristics are still traceable in the summer circulation.

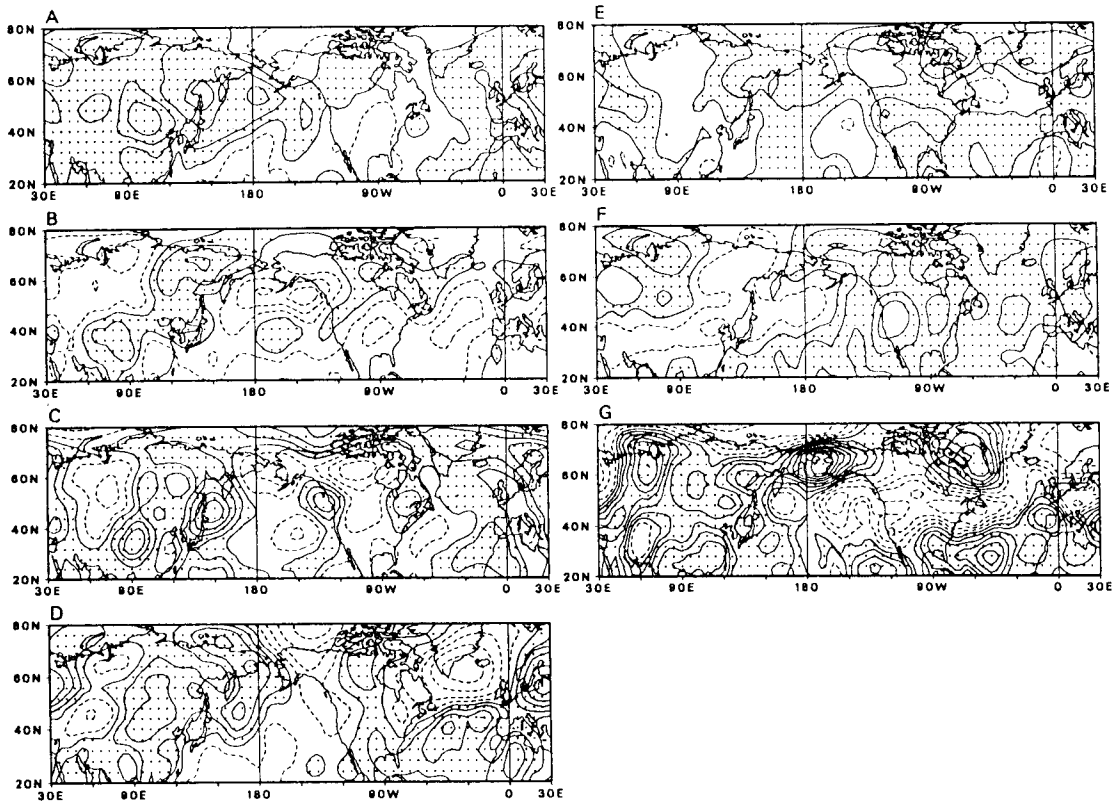

Fig. 7. As in Figure 5, but for July 300-700 mb thickness.

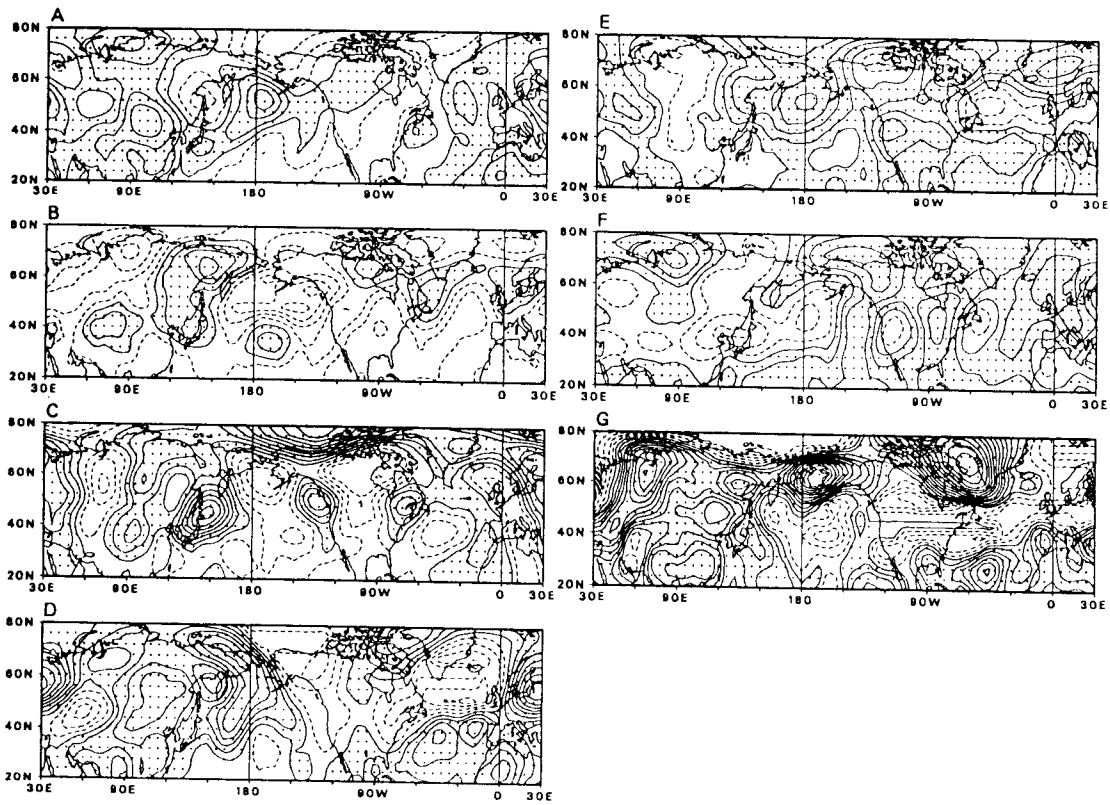

Fig. 8. Anomaly fields of July 300 mb Z associated with different types of SST anomalies during the period of 1955-93. Solid lines are for zero and positive, and dashed lines for negative. The contour interval is 10 m.

4. Principal components of the Northern Hemisphere circulation

The Northern Hemisphere climate of the last two decades has been characterized by recurring major ENSO events. The tabulation of SST types in Table 2 indicates that F, E and C types dominate this period to the present. These types are related to ENSO events to various degrees. During the most recent three years, the persistent major ENSO episodes and associated F type SST patterns are particularly noteworthy.

A principal component analysis is performed for the SST data from July 1991 to December 1993. The pattern vectors are shown in Figure 9 for 1st to 4th components. Unlike the principal component analysis of 36 years as presented in Kung *et al.* (1994), this analysis does not eliminate the intra-annual seasonal variation and uses the entire 30- month mean as the basis of calculating anomalies. The 1st component as shown in Figure 9 corresponds to the seasonal variation as reported in Figure 4 of Kung *et al.* (1994). It is noted that the positive and negative in pattern vectors of principal components in Figure 9 are reversed from general patterns in Figure 4 of Kung *et al.* (1994). Signs of pattern vectors are given arbitrarily by the computer software, and need not be concerned (Preisendorfer, 1988).

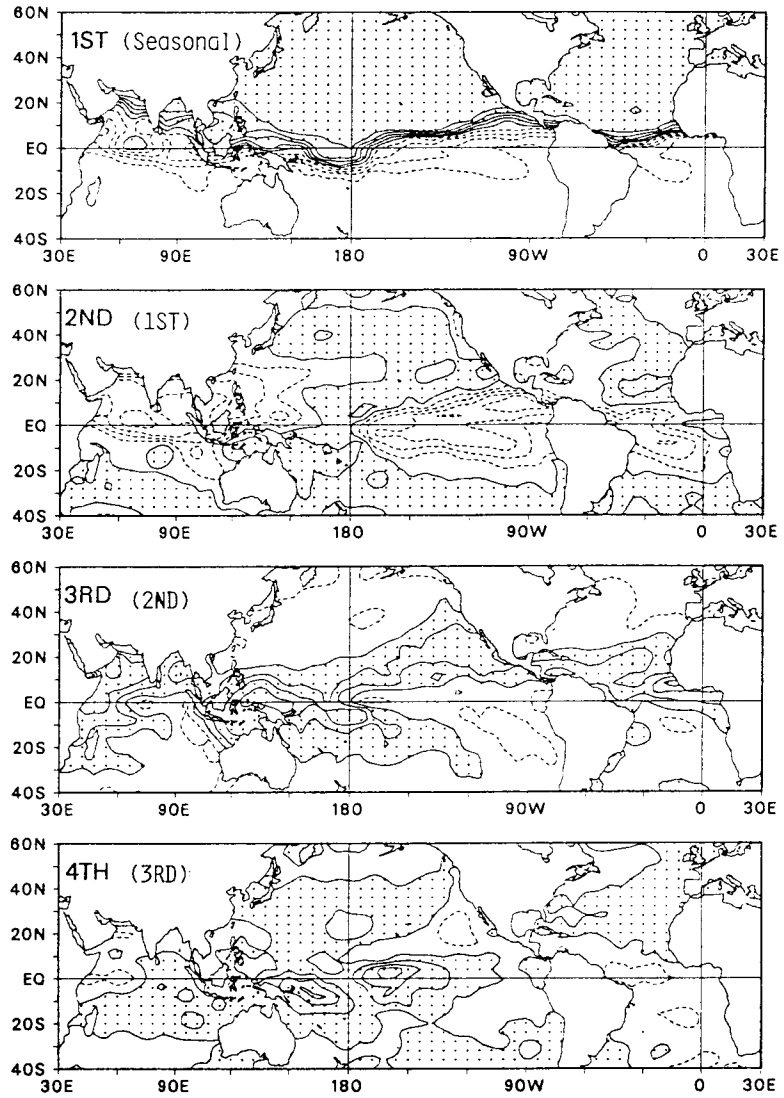

Fig. 9. Characteristic patterns for the first four principal components of monthly SSTs for the 30-month period from July 1991 to December 1993. The contour interval is 0.2. The identification of components in parentheses is the order after elimination of the 1st component which is the intra- annual seasonal variation.

The 2nd component in Figure 9, which is the 1st component after elimination of the seasonal variation, is comparable to the 1st component of long-term SST patterns (Kung *et al.*, 1994). However, this component in the recent three years is much better defined than the long-term patterns in the tropics, particularly in the eastern tropical Pacific and tropical Atlantic. On the contrary, the 3rd component is significantly weaker than the comparable 2nd component found in the long-term patterns. However, a well defined subtropical to mid-latitude pattern of the southwest-northeast orientation of the 3rd component is shown in the Pacific and Atlantic north of the intensified tropical portion for the 2nd component. The 4th component is also less intense than the comparable 3rd component of the long-term patterns. The ENSO- dominated climate

of the most recent three years is thus associated with the exceptionally strong anomalies in the tropical ocean and subtropical to mid-latitude SST patterns, respectively shown in the 2nd and 3rd components (i.e., the 1st and 2nd component after elimination of the intra-annual seasonal component).

5. Utilities of ENI in the long-range forecasting

As often ENSO episodes are associated with the extremely anomalous Northern Hemisphere circulation, an index to describe ENSO occurrence may have practical value as a parameter for long-range forecasting. Not only is the index meaningful for the ENSO occurrence, but it also may provide an indication for various levels of ENSO-related modes of the forcing, thus indicating various patterns of SST anomalies. In the long-term analysis of SST for the period of 1955-1992, Kung *et al.* (1994) found that coefficients of both 1st and 2nd components mark the occurrence of ENSO events. For the general use as a predictor at a seasonal range, we define ENI as the weighted mean of the coefficients of the 1st and 2nd components during the period of 1955-1993 by their respective variances.

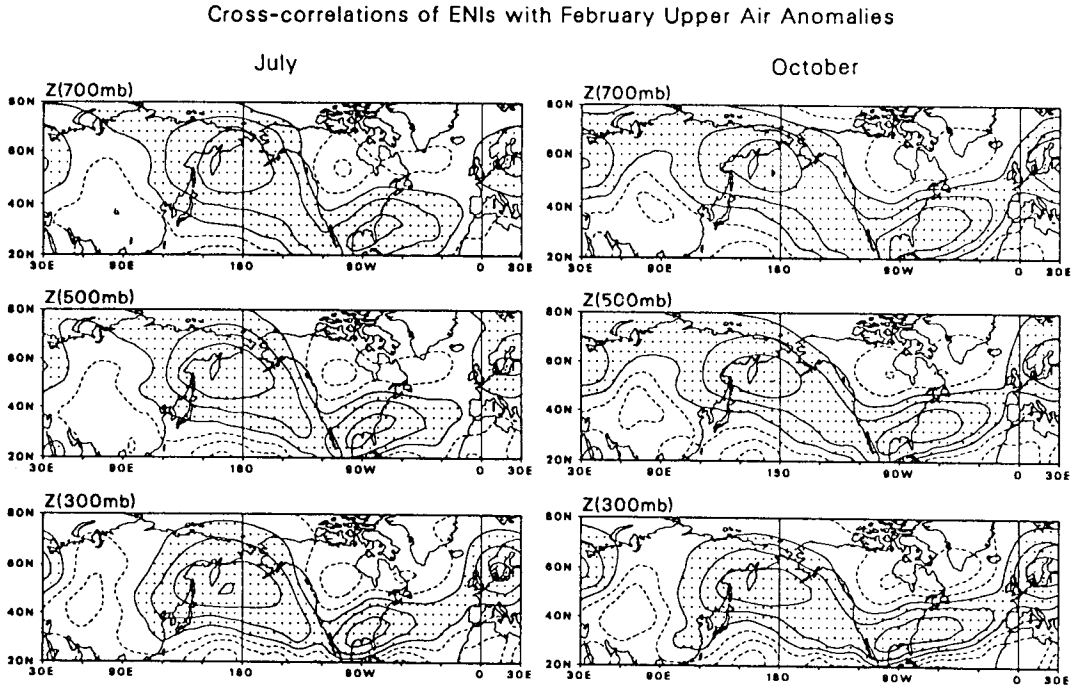

Fig. 10. Cross-correlations of July and October ENIs with following February upper air circulations. The contour interval is 0.2.

Figures 10 and 11 are cross-correlation patterns between preceding ENIs and following monthly means of tropospheric circulations in terms of Z at 700, 500 and 300 mb. Figure 10 is for the July and October ENIs and the following February circulation, and Figure 11 for the January and April ENIs and the following June circulation. The interval of the contour lines is 0.2 and the first contour is the 0 line. For the period of 38 years (1955-1992), the temporal correlation coefficient 0.3 is significant at 95% level, 0.4 at 99% level, and 0.5 at 99.9% level. It is immediately

noted that the correlation patterns are consistent through the troposphere from 700 mb to 300 mb. The centers of defined areas of correlation are very significant, lending to the meaningfulness of correlation patterns. The patterns are also consistent for ENIs through at least two seasons preceding the circulation, clearly indicating the usefulness of defined ENI as a predictor at the seasonal range. The correlations are stronger with the winter circulation (Fig. 10) than with the summer circulation (Fig. 11). However, even for the latter pattern and meaningfulness of the correlation patterns for the long-range forecasting are clear. The significance of correlations as presented in Figures 10 and 11 is at least partially due to the long characteristic time of SSTs or persistence of SST anomalies. Ability of ENIs to represent the variation of SST patterns is a subject of further study. It will be pertinent to note that, once the use of ENIs as a predictor is established, it can be used in conjunction with the SST prediction model (Adem, 1970; Adem *et al.*, 1994) for the construction of numerical-empirical seasonal-range prediction scheme.

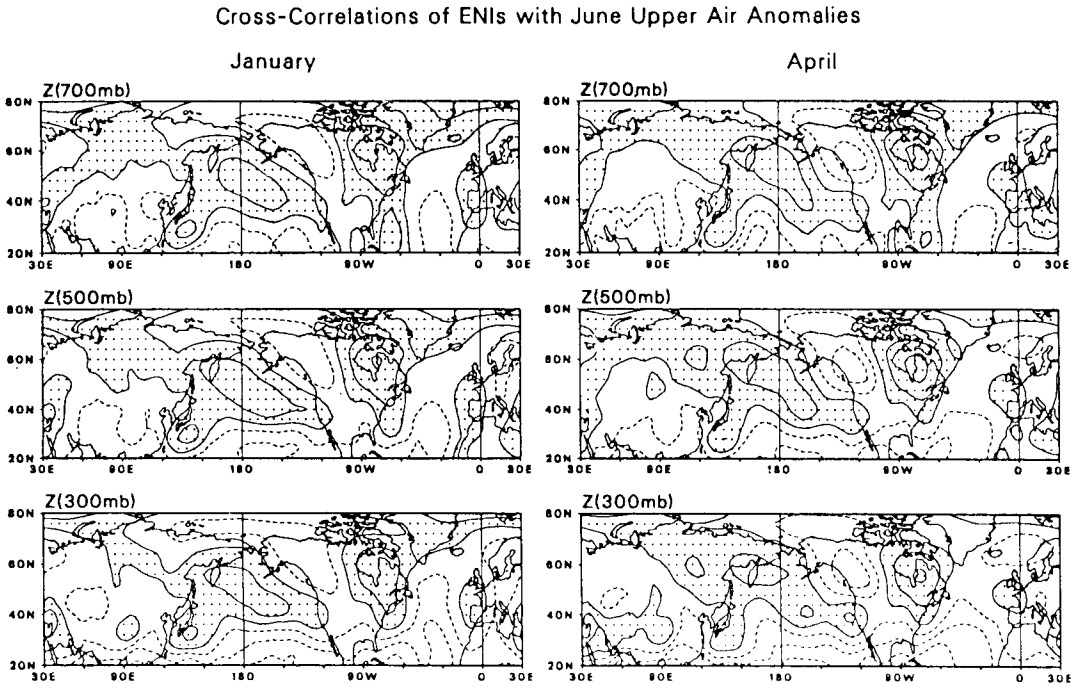

Fig. 11. As in Fig. 10, but for January and April ENIs with the following June upper air circulations.

6. Concluding remarks

Following our preceding study (Kung *et al.*, 1994) on principal components of the global SSTs, a synoptic classification of SST patterns is presented for ready recognition of prevailing SST patterns without invoking principal component analysis. The observed monthly anomalies of the global SSTs during the 39-year records indicate the shift of climate patterns in response to prevailing SSTs. Since the late 1970s there is a drastic increase of SST types which are related with ENSO events, the peak of which characterizes the current prevailing climate pattern. The responding tropospheric circulations to these SST types are presented, and explained in terms of *in site* warming and dynamic nonlinear transformation of energy.

Further, a principal component analysis is performed for the most recent 30-month SSTs up to December 1993 to analyze the recent few years' forcing of major persistent ENSO events. The most recent years' ENSO dominance is associated with extremely strong 1st component after elimination of the seasonal component and a clear southwest-northeast orientation of the 2nd component north of the intensified tropical portion of the 1st component.

Utilities of ENSO parameters in the seasonal range forecasting is demonstrated with ENI (El Niño Index), which is defined as the weighted means of the coefficients of 1st and 2nd principal components. The cross-correlation between the Northern Hemisphere circulation and preceding ENIs clearly indicate the seasonal range predictability of the Northern Hemisphere circulation.

Acknowledgements

The authors are grateful to Ms. D. C. Marsico of the National Meteorological Center for providing the NMC SST analyses, and to Ms. Tanya Henke for providing technical assistance.

REFERENCES

Adem, J., 1970. On the prediction of mean monthly ocean temperatures. *Tellus*, 22, 410-430.

Adem, J., E. E. Villanueva and V. M. Mendoza, 1994. Preliminary experiments on the prediction of sea surface temperature anomalies in the Gulf of Mexico. *Geofís. Int.*, **33**, 511-521.

DaCamara, C. C., E. C. Kung, W. E. Baker, B.-C. Lee, and J. A. M. Corte- Real, 1992. Long term analysis of planetary wave activities and blocking circulation in the Northern Hemisphere winter. *Beit. Phy. Atmos.*, **64**, 285-298.

Fukunaga, K., 1972. *Introduction to Statistical Pattern Recognition.* Academic Press, 369 pp.

Halpert, M. S., G. D. Bell, V. E. Kousky and C. F. Ropelewski, Eds., 1994. *Fifth Annual Climate Assessment 1993.* Climate Analysis Center/NMC/NWS/NOAA, 111 pp.

Hartman, D. L. and S. J. Ghan, 1980. A statistical study of the dynamics of blocking. *Mon. Wea. Rev.*, **108**, 1144-1159.

Houghton, J. T., G. I. Jenkins and J. J. Ephraums, Eds., 1990. *Climate Change–The IPCC Scientific Assessment.* Cambridge Univ. Press, 366 pp.

Houghton, J. T., B. A. Chandler and S. K. Varney, Eds., 1992. *Climate Change 1992–The Supplementary Report to the IPCC Scientific Assessment.* Cambridge Univ. Press, 200 pp.

Kung, E. C., and W. E. Baker, 1986. Spectral energetics of the observed and simulated Northern Hemisphere general circulation during blocking periods. *J. Atmos. Sci.*, **43**, 2792-2812.

Kung, E. C., and J. Susskind and C. C. DaCamara, 1993. Prominent Northern Hemisphere winter blocking episodes and associated anomaly fields of sea surface temperatures. *Terrestrial, Atmospheric and Ocean Sciences*, **4**, 273-291.

Kung, E. C., J.-G. Chern and J. Susskind, 1994. Large-scale mode of variations in the global sea surface temperatures and Northern Hemisphere tropospheric circulation. *Atmósfera*, **7**, 143-158.

Preisendorfer, R. W., 1988. *Principal Component Analysis in Meteorology and Oceanography.* Elsevier, 425 pp.

World Meteorological Organization/World Climate Data and Monitoring Programme, 1991. *The Global Climate System. Climate System Monitoring December 1988-May 1991.* 110 pp.